AIAA 98-2808

Turbularization of the Stokes Layer Over a Transpiring Surface

J. Barron and W. K. Van Moorhem
University of Utah
Salt Lake City, UT 84112

J. Majdalani
Marquette University
Milwaukee, WI 53233

29th AIAA Fluid Dynamics Conference
June 15–18, 1998 / Albuquerque, NM

Turbularization of the Stokes Layer Over a Transpiring Surface

J. Barron* and W. K. Van Moorhem†
University of Utah, Salt Lake City, UT 84112
and
J. Majdalani‡
Marquette University, Milwaukee, WI 53233

In this work, the onset of turbulence inside a rectangular chamber is investigated, with and without side-wall injection, in the presence of an oscillatory pressure gradient. Three techniques are used to define the transition from laminar to turbulent regimes: statistical analysis, spectral analysis, and flow visualization. Calibrated hot film anemometry and a computer data acquisition system are used to record and analyze acoustic flow data. Four classifications of flow regimes are achieved: (a) laminar, (b) distorted laminar, (3) weakly turbulent, and (4) conditionally turbulent. A fully turbulent flow could not develop at any of the driving frequencies tested. A relaminarization always occurs within a cycle. Transition between flow regimes is assessed from the standard deviation of velocity data correlated as a function of acoustic Reynolds number. Transition in oscillatory flow with side-wall injection is found to be reproducible at the same critical value of the acoustic Reynolds number, Re_A = 195.

I. Introduction

In a rocket motor, acoustic oscillations can affect the burning rate of the propellant, leading to combustion instabilities. It is very difficult and expensive to study experimentally the behavior of oscillatory burning in solid propellant motors. For this reason, a simulation facility was constructed that uses solid carbon dioxide (dry ice) to simulate the internal flow field of a solid propellant rocket motor. The use of dry ice makes it possible to study the fluid mechanical aspect of rocket motors without combustion. The research includes modifying an existing simulation facility to improve certain experimental deficiencies and implementing new experimental techniques. The work involves quantifying the occurrence of acoustically introduced turbularization and investigating flow phenomena that may contribute to possible acoustic instability sources.

The mechanisms that trigger turbulence in steady flows are reasonably well understood. The main criterion for predicting turbulent regimes is based on the Reynolds number which roughly scales the ratio of inertial to viscous forces affecting the main flow. Transition Reynolds numbers based on the characteristic dimension of the main steady flow are more or less well defined. While prediction of turbulent regimes in steady flows has been studied considerably during the past century, the problem of predicting turbulence in unsteady periodic flows remains unresolved. On that account, this work will attempt to address some unresolved features of unsteady periodic flows as one of its main objectives.

A variety of problems involving turbulent oscillatory flows are frequently encountered in the applied fields of fluid mechanics. One recent topic is closely related to the study of combustion instability in solid rocket motors. An acoustic boundary layer or Stokes layer results from an oscillatory flow over a solid boundary that satisfies the no-slip condition. The instability of the Stokes layer has been investigated by several researchers.[1-9] However, previous experiments have been limited to the study of transitional behavior of the Stokes layer over a nontranspiring surface. Under this condition, the thickness of the Stokes layer, δ, was given as $\sqrt{2\nu/\omega}$, where ν and ω are the kinematic viscosity and circular frequency of the oscillations. Early investigators discovered that the onset of turbulence is governed by the Reynolds number based on the thickness of the boundary layer, $\mathrm{Re}_\delta = \delta U_0/\nu$,

*Currently Head of Mechanical Engineering, Halff Associates, Inc., Dallas, TX 75225. Member AIAA.

†Professor, Department of Mechanical Engineering. Senior Member AIAA.

‡Assistant Professor, Department of Mechanical and Industrial Engineering. Member AIAA.

which is also known as the acoustic Reynolds number when written in the form:

$$\mathrm{Re}_A = \sqrt{\pi}\,\mathrm{Re}_\delta = U_0 \Big/ \sqrt{f\nu} \qquad (1)$$

In Eq. (1), U_0 is the amplitude of the oscillatory axial velocity component and f is the frequency of oscillations.

Transpiring surfaces are surfaces that exhibit the characteristics of combusting solid boundaries, such as burning solid propellants, often modeled as porous surfaces with side-wall injection. From the fluid mechanics point of view, all parameters used to characterize periodic flows remain valid here. One more parameter of fundamental importance that makes its appearance here is the injection speed at the wall. The problem of predicting turbulence in this case will hence depend on the injection Reynolds number as well (based on the Stokes layer thickness and the injection velocity of the fluid). In this dry-ice experiment, the sublimation rate of solid CO_2 is dependent upon the heat input, exhibiting similar characteristics to normal solid propellants. The experimental work carried out by Ma[10] constitutes the only meaningful empirical research found in the literature.

Beddini and Roberts[11-13] investigated the onset of acoustically generated turbulence by numerical simulations. Their results indicate that, for an isothermal flow (with no initial disturbance and a perfectly smooth wall), low injection velocities initially decrease the acoustic amplitude needed for transition (from the no-injection case). This makes intuitive sense as one would expect injection to promote turbulence in the system. As the injection velocity increases, the acoustic amplitude required for transition passes through a minimum and increases to a value similar to that in the no-injection case. If there is initial turbulence in the medium, the minimum may not exist and the required acoustic amplitude may continue to decrease from the no-injection case.

II. Experimental Apparatus

The Solid Carbon Dioxide Simulation Facility is a cold flow (nonreactive) facility. The use of solid carbon dioxide (CO_2 or dry ice) as the simulated propellant makes it possible to focus on the fluid mechanics of the acoustic instability problem by separating the fluid mechanics from the combustion dynamics at the propellant surface. The Solid Propellant Rocket Motor Simulation Facility used in these experiments is shown in Figure 1. The flow chamber has a square cross section with an inside dimension of 7.62 by 7.62 centimeters. The flow chamber consists of eight interchangeable sections, a

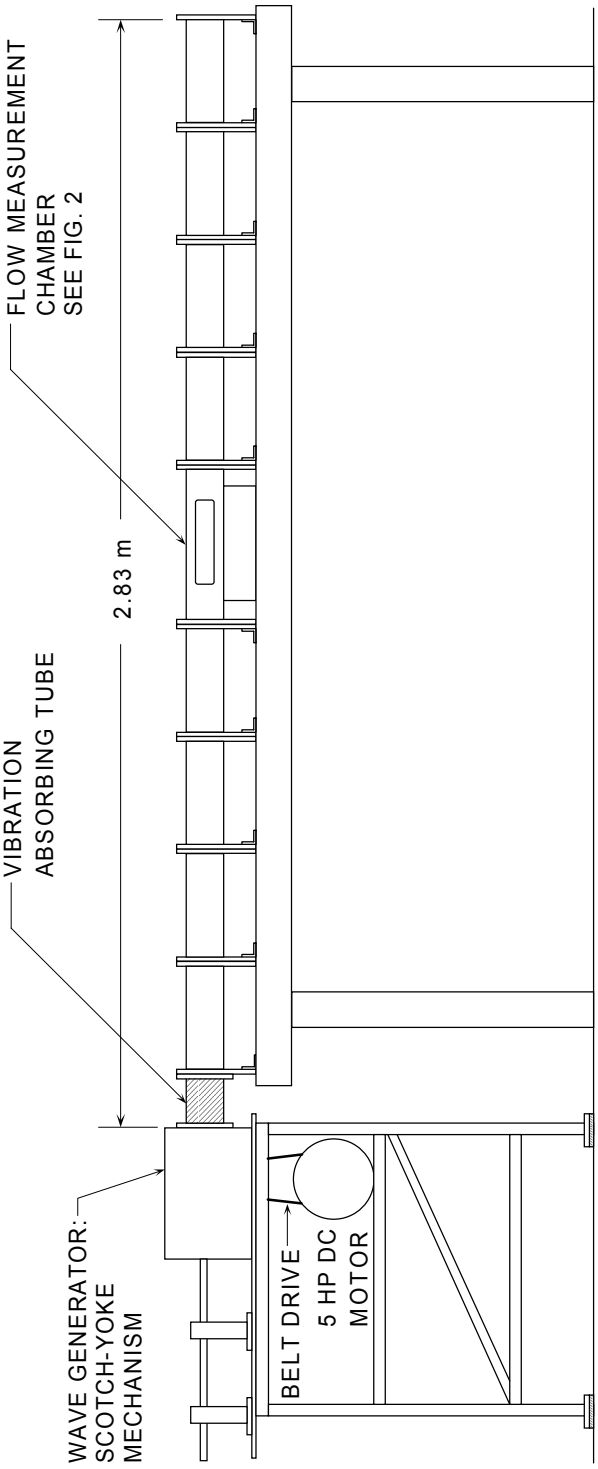

Fig. 1 Experimental apparatus.

test section used for flow measurement, and a vibration isolating tube. The entire flow chamber is bolted to a heavy granite table to minimize vibration. The interchangeable sections make it possible to vary the test section location, chamber length and system resonant frequency. For these experiments, the length was held constant at 2.83 meters corresponding to a

resonant frequency of 49 Hz at a temperature of 27 ^{o}C. For all experiments, the chamber was initially purged with room temperature CO_2 gas to remove the air. The CO_2 gas enters at one end of the flow chamber and exits the chamber at the opposite end through a small orifice which is closed with a valve prior to operating the wave generator.

The center section of the flow chamber is a 43.2 cm long test section (see Figure 1). The test section was placed near the center of the chamber where the acoustic velocity antinode (maximum velocity) occurs and a pressure node (pressure minimum) occurs for a standing wave. This setup minimizes any pressure type of coupling in the dry ice sublimation. Figure 2 shows a section view of the test section. Solid carbon dioxide (dry ice) is used in the test section to simulate solid propellant rocket motor characteristics. The sublimation of the solid CO_2 into gaseous carbon dioxide simulates the burning of the propellant. The solid CO_2 is a commercial dry ice block approximately 30 cm long, 5 cm deep, and 7.62 cm in width which is equal to the width of the test section. The dry ice rests on a wooden block and a bellows is used to maintain the top of the dry ice at the same level as the bottom of the test section. The bellows pushes the dry ice with a constant supply air pressure of 3 psig. The bellows supply pressure is sufficiently large to eliminate significant vibration of the dry ice block due to acoustic pressure oscillations on the top dry ice surface. The dry ice can be replaced with a fitted aluminum plate that makes the investigation of the flow field without side-wall injection possible. Glass view ports are located on either side of the test section to facilitate visual flow monitoring. The velocity of the gas near the surface of the dry ice can be measured by hot film anemometry. A hot film anemometer is mounted in the test section in order to measure local velocities. The hot film probe is centered above the dry ice and is located approximately 0.8 cm above the surface of the dry ice. The hot film probe is mounted perpendicular to the dry ice surface.

Pressure oscillations in the flow chamber can also be measured. A pressure transducer can be mounted at various locations in the chamber to record the pressure oscillations. For these experiments the pressure transducer was located at the end of the flow chamber opposite the wave generator where maximum pressure is observed.

The sublimation of solid CO_2 was chosen over previously used simulation techniques for several reasons. Although weaker, the dynamic behavior of the solid CO_2 is analogous to the behavior of actual propellant. In a rocket motor, increasing the pressure results in an increase in propellant burn rate and mass flow rate. Similarly, an increase in the pressure over the solid CO_2 results in an increase in the sublimation rate and therefore mass flow from the surface. This

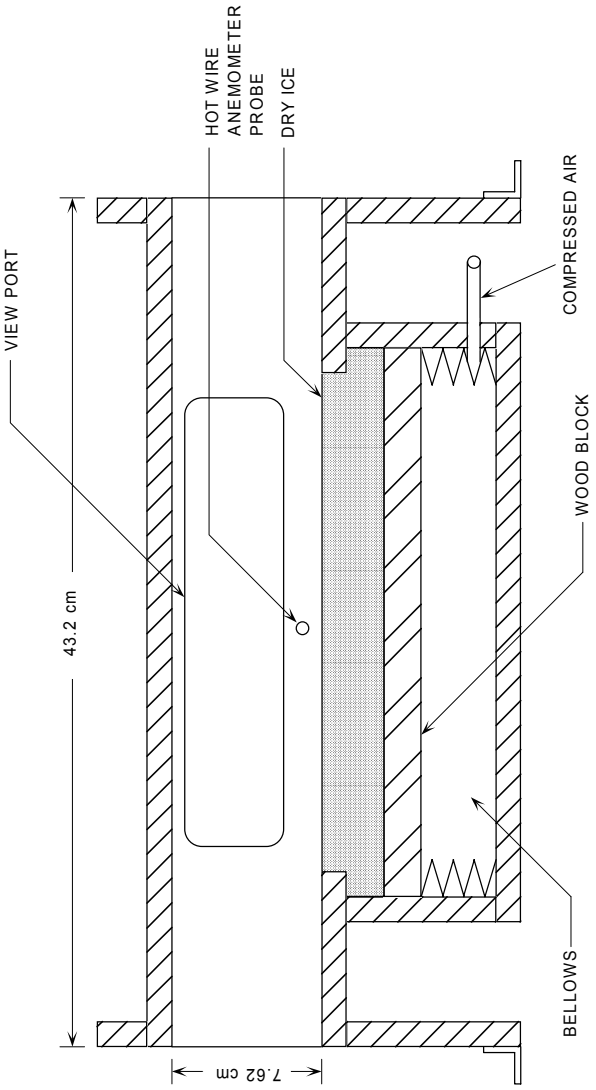

Fig. 2 Flow measurement chamber.

increase is due to the decrease in the heat of sublimation with increasing pressure. Other cold flow facilities usually simulate the combustion process by injecting gas through a porous wall. The pores must be choked to prevent acoustic energy from being lost into the wall. An increase in pressure above the porous wall results in either unchoking of the pores and decreasing the mass flow or a constant mass flow rate if the pores remain choked. Neither of these mechanisms simulate actual propellants. An even more serious problem is the possibility that the injection process itself causes turbulence. The use of solid CO_2 eliminates the question of choking or not choking at the pores and makes it ideally suited for simulating the behavior of a solid rocket motor propellant.

Several modifications were implemented as improvements to the experiments done by others. An experimental difficulty in Ma's[10] experiments was that a slider-crank mechanism, with a crankshaft,

connecting rod and piston was used to generate the acoustic environment. The slider-crank driving system complicated the flow data by adding undesirable harmonics. A scotch yoke mechanism was designed and constructed to provide a purer sinusoidal piston motion. The scotch yoke piston motion provided acoustic flow data which was not complicated by additional harmonics, facilitating a meaningful method of performing statistical analysis. The pressure and velocity data acquired in the experiments was Fourier analyzed to demonstrate the reliability of the driving mechanism.

Two oscillatory flow conditions were investigated in a rectangular chamber purged with CO_2 gas. The two conditions are: (1) oscillatory flow with side-wall injection and (2) oscillatory flow without side-wall injection. Solid CO_2 (dry ice) is used to simulate side-wall injection which occurs in the burning of propellant in the oscillatory flow inside an unstable solid propellant rocket motor. Experiments with side-wall injection were performed for driving frequencies between 2.2 and 50.8 Hz which result in an Re_A (acoustic Reynolds number) ranging between 83 and 2150. Experiments without side-wall injection were performed for driving frequencies between 2.3 and 44.8 Hz which result in an Re_A ranging between 55 and 500. Four types of flow regimes were observed: laminar, distorted laminar, weakly turbulent, and conditionally turbulent.

III. Transition to Turbulence

Three different methods were implemented to determine the occurrence of turbulence: statistical analysis of acoustic flow data, spectral analysis of acoustic flow data, and flow visualization. The statistical analysis of acoustic flow data provides a method of quantifying the occurrence of turbulence.

A. Statistical Analysis

The statistical data provides a method of determining not only if turbulence occurs but also during what parts of the oscillating cycle the flow remains turbulent. For detailed modeling of oscillatory flow, it is important to determine how turbulence occurs and if the flow returns to laminar conditions during an oscillatory cycle. A large standard deviation relative to the velocity magnitude is assumed to be indicative of turbulent flow.

Maximum standard deviation as a function of acoustic Reynolds number for experiments without side-wall injection is shown in Figure 3. For $Re_A < 110$ the flow is laminar. An almost linear power law relationship appears to exist between the standard deviation and the Reynolds number. This relationship is of the form $\sigma = a\mathrm{Re}_A^b$, where σ is the standard deviation and a and b are constants. The power law coefficient is 2.1 for the laminar case. The standard deviation of the laminar flow is very small (approximately 4% of the maximum velocity amplitude). Distorted laminar flow is observed at an Re_A between 110 and 273. The largest standard deviations occur in the accelerating and decelerating phases in this regime. The standard deviation for distorted laminar flow is slightly larger than for laminar flow. Weakly turbulent flow is observed at $Re_A = 273$. The standard deviations are larger than those for the laminar or distorted laminar cases and the maximum standard deviation occurs at the velocity peaks. A slightly smaller standard deviation is observed in the accelerating phase where the turbulence is generated. Relaminarization occurs during the same cycle during the decelerating phase. The largest standard deviation without side-wall injection occurs in the $Re_A = 500$ case in which conditionally turbulent flow is achieved. In this regime, the maximum standard deviation occurs in the decelerating phase where turbulence is generated. In the conditionally turbulent regime, turbulent bursts occur just after the velocity peaks in the decelerating phase. These turbulent bursts are identified by a large standard deviation that appears suddenly, persists for a short time, and then decreases rapidly as the flow returns to laminar. As seen in Figure 3, the power law coefficient b relating σ to Re_A decreases from 2.1 to about 1.2 in the region corresponding to $Re_A = 110$, where turbulence begins to grow.

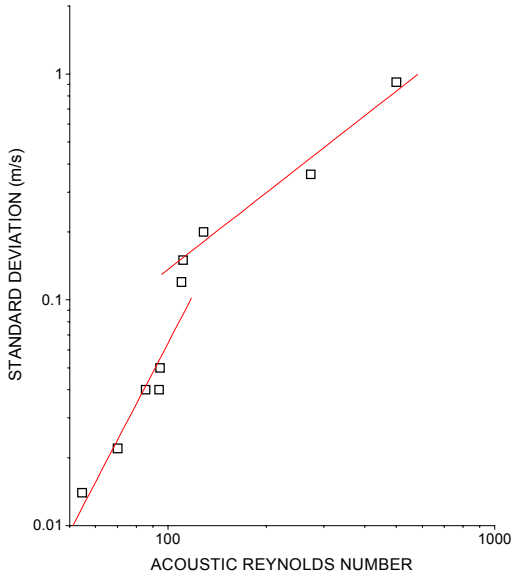

Fig. 3 Standard deviation vs. acoustic Reynolds number Re_A for experiments without side-wall injection.

Maximum standard deviation as a function of acoustic Reynolds number for experiments with side-wall injection is shown in Figure 4. For $Re_A < 142$ the flow is laminar. An almost linear power law relationship also appears to exist between the standard deviation and the acoustic Reynolds number for the side-wall injection case. The power law coefficient is 2.6 for the laminar case. The standard deviation of the laminar flow is very small (approximately 4% of the maximum velocity amplitude). Distorted laminar flow is observed at an Re_A between 142 and 195. The largest standard deviations occurs in the accelerating and decelerating phases. The standard deviation for distorted laminar flow is slightly larger than for laminar flow. Weakly turbulent flow is observed at $Re_A = 195$ and $Re_A = 302$. The maximum standard deviation in this regime occurs at the velocity peaks and a slightly smaller standard deviation is observed in the accelerating phase where the turbulence is generated. The standard deviation becomes small during the decelerating phase when relaminarization occurs. Conditionally turbulent flow is observed at $Re_A = 677$ and $Re_A = 2150$. In this regime, the maximum standard deviation occurs in the decelerating phase where turbulence is generated. In the conditionally turbulent regime, turbulent bursts occur just after the velocity peaks in the decelerating phase. These turbulent bursts are identified by a large standard deviation that appears suddenly, persists for a short time, and then decreases rapidly as the flow returns to laminar. At $Re_A = 2150$, the flow is turbulent during most of the cycle; however, fully turbulent flow was not observed in any of the experiments. In every case, flow was either laminar or relaminarization occurred during some part of the oscillatory cycle. As seen in Figure 4, the power law coefficient b relating σ to Re_A decreases from 2.6 to about 1.1 in the region corresponding to $Re_A = 195$, where turbulence begins to dominate during a cycle.

B. Spectral Analysis

The occurrence of turbulent flow can be identified by a broad band spectrum of velocity data measured by hot film anemometry. The occurrence of turbulence first appears in the low frequency band (0-100 Hz) since most turbulent energy is carried by large scale eddies. It is also important to look for broad band regions in higher frequencies to identify the occurrence of high frequency turbulent bursts which can be observed primarily in the conditionally turbulent flow. Since the primary motion of the gas in the flow chamber is oscillatory, the resulting frequency spectrum will always be dominated by the driving frequency and any harmonics of the driving piston or the flow chamber itself that are excited.

For laminar and unsteady laminar flows, a Fourier analysis shows that the velocity spectra is made up

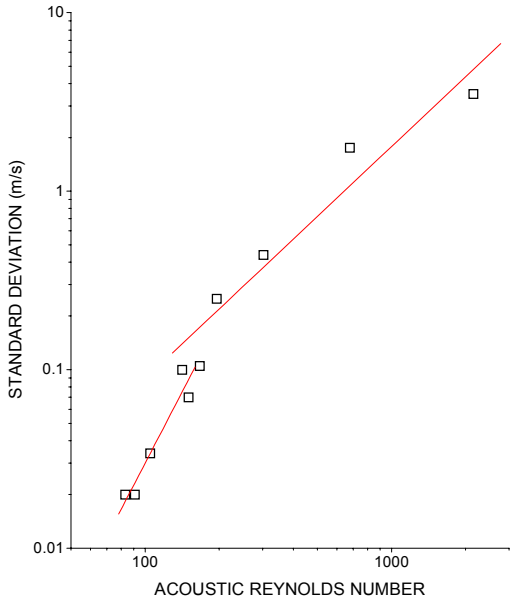

Fig. 4 Standard deviation vs. acoustic Reynolds number Re_A for experiments with side-wall injection.

almost entirely of the piston driving frequency. For the unsteady laminar case, the fundamental and harmonic frequencies of the chamber are also present. For weakly turbulent and conditionally turbulent flows, a Fourier analysis indicates that the largest frequency component in the velocity spectra is still due to the driving frequency. However, the frequency spectrum for turbulent flows is broader with significant contributions at many frequencies which is indicative of turbulent flow.

C. Flow Visualization

Flow visualization was used to examine flow characteristics in experiments with dry ice in the test section. Under steady state operating conditions, a fog-like layer can be seen above the dry ice which is caused by water (approximately 1% by weight) used to bind the dry ice together during the manufacturing process. The behavior of the "fog" in the flow chamber can be useful in qualitatively determining the critical Reynolds number at which transition to turbulence occurs. The flow is considered turbulent when the flow field exhibits high intensity mixing and solid CO_2 particles leave the dry ice surface due to local high intensity instability. Flow visualization is the least conclusive method of detecting turbulence since the analysis is qualitative and the results are somewhat subjective.

The fog layer appears to be uniform across the test section for driving frequencies less than 30 Hz ($Re_A < 195$). The flow also appears to be stable with no

indication of mixing. At approximately 30 Hz (Re_A = 195), solid CO_2 particles are observed to leave the dry ice surface due to local high intensity instability. For driving frequencies above 30 Hz, the two-dimensional wave propagation is no longer present. The fog layer motion is chaotic and three-dimensional. At driving frequencies greater than 30 Hz, the flow appears to be turbulent. As the driving frequency is varied from 30 Hz to 45 Hz (Re_A = 195 to 1020), the number of particles ejected from the dry ice surface into the flow field increases and mixing becomes more intense with increasing driving frequency. For flow above approximately a 40 Hz driving frequency (Re_A = 650) the "fog" is no longer visible due to intense mixing. From flow visualization, the critical frequency for transition to turbulence is approximately 30 Hz which is in good agreement with the statistical analysis of the hot film anemometry data. Weakly turbulent flow is first seen at 30.4 Hz (Re_A = 195) in the statistical analysis.

Summary

Several experimental deficiencies of previous researchers were improved in these experiments. An experimental apparatus that incorporated a nearly pure harmonic wave generator has been successfully constructed and implemented. Undesirable harmonics produced by a typical slider-crank mechanism (used in previous experiments) have been minimized after substitution by a Scotch yoke mechanism. A data acquisition system controlled by a computer was implemented which was capable of collecting many samples of acoustic velocity and pressure data at consecutive cycles at the same driving frequency. The method of data collection facilitated statistical and spectral analysis of the acoustic data.

The onset of turbulence has been investigated for an oscillating flow in a rectangular geometry with and without side-wall injection. Side-wall injection at the transpiring surface was achieved by using sublimating dry ice. Sublimating dry ice exhibits many desirable features such as its ability to simulate the burning of a solid rocket propellant, its noninterference with the natural system frequency, its resistance to acoustic dissipation (through pores found in other traditional cold-flow experiments incorporating side-wall injection) and its safe handling advantages. Calibrated hot film anemometry was used to record the velocity amplitude near the dry ice surface. Three techniques were used to define the transition from laminar to turbulent regimes: statistical analysis, spectral analysis, and flow visualization. The structure of turbulence in time-dependent flow has been investigated using computer data collection and hot film anemometry.

Hino[6] and coworkers classified four distinct flow categories in their experiments. These were: (a) laminar, (b) distorted laminar, (c) weakly turbulent, and (d) conditionally turbulent regimes. The flow structures observed in the current experiments were classified into these four categories.

The statistical flow analysis showed that the fully turbulent flow regime was not developed even at the highest frequencies permitted by the wave generator. In agreement with other investigations, a relaminarization occurred within every cycle when the velocity amplitude diminished below a certain value.

Through flow visualization, transition in oscillatory flow with side-wall injection was found to be reproducible and repeatable at the same critical value of the acoustic Reynolds number, Re_A = 195.

References

[1]Vincent, G. E., "Contribution to the Study of Sediment Transport on a Horizontal Bed due to Wave Action," *Proceedings of Conference on Coastal Engineering*, University of Florida, Vol. 16, 1957, pp. 326-335.

[2]Collins, J. I., "Inception of Turbulence at the Bed Under Periodic Gravity Waves," *Journal of Geophysical Research*, Vol. 68, 1963, pp. 6007-6014.

[3]Sergeev, S. I., "Fluid Oscillations in Pipes at Moderate Reynolds Numbers," *Fluid Dynamics*, Vol. 1, 1966, pp. 21-22.

[4]Li, H., "Stability of Oscillatory Laminar Flow Along a Wall," Beach Erosion Board, U.S. Army Corps of Engineers, Washington, D.C., Tech. Memo. No. 47, 1954.

[5]Merkli, P., and Thomann, H., "Transition to Turbulence in Oscillating Pipe Flow," *Journal of Fluid Mechanics*, Vol. 68, 1975, pp. 567-575.

[6]Hino, M., and Sawamoto, M., "Linear Stability Analysis of an Oscillatory Flow Between Parallel Plates," *Proceedings of the 7th Symposium on Turbulence*, 1975, pp. 1-7.

[7]Hino, M., Kashiwayanagi, M., Nakayama, A., and Hara, T., "Experiments on the Turbulence Statistics and the Structure of a Reciprocating Oscillatory Flow," *Journal of Fluid Mechanics*, Vol. 131, 1983, pp. 193-207.

[8]Ohmi, M., Iguchi, M., Kakehashi, K. and Masuda, T., "Transition to Turbulence and Velocity Distribution in an Oscillating Pipe Flow," *Bulletin of the JSME*, Vol. 25, 1982, pp. 365-371.

[9]Akhavan-Alizadeh, R., "An Investigation of Transition and Turbulence in Oscillatory Stokes Layers," Ph. D. Dissertation, Department of Mechanical Engineering, MIT, 1987.

[10]Ma, Y., "A Simulation of the Flow Near a Burning Propellant in a Solid Propellant Rocket Motor," Ph. D. Dissertation, Department of Mechanical Engineering, University of Utah, 1990.

[11]Beddini, R. A., and Roberts, T. A., "Turbularization of an Acoustic Boundary-Layer on a Transpiring Surface," AIAA Paper 86-1448, 22nd AIAA Joint Propulsion Conference, June, 1986.

[12]Beddini, R. A., and Roberts, T. A., "Response of Propellant Combustion to a Turbulent Acoustic Boundary Layer," AIAA Paper 88-2942, 24th AIAA Joint Propulsion Conference, July, 1988.

[13]Roberts, T. A., and Beddini, R. A., "A Comparison of Acoustic and Steady-State Erosive Burning in Solid Rocket Motors," AIAA Paper 89-2664, 25th AIAA Joint Propulsion Conference, July, 1989.